Measurement 122 (2018) 168–177

Contents lists available at ScienceDirect

Measurement

journal homepage: www.elsevier.com/locate/measurement

The importance of meteorological variation on PPP positioning

Nedim Onur Aykut

Yildiz Technical University, Department of Geomatic Engineering, Davutpasa/Esenler, Istanbul, Turkey

ARTICLE INFO

Keywords:
GNSS/GPS
PPP
RMS
Meteorological
Seasonal

ABSTRACT

The Precise Point Positioning (PPP) technique has been used in many engineering applications. After using online PPP web services, researchers have increasingly taken the opportunity to study this technique. PPP is a positioning technique aimed at processing measurements from a single GNSS receiver in order to compute a highly accurate position in a global reference frame.

The purpose of this study is to determine the effects of meteorological variations on the accuracy of PPP positioning. The Canadian Spatial Reference System (CSRS) – one of the most popular online web services – was selected for processing data from 36 observation days in 2014 acquired from the YLDZ reference station. Furthermore, the meteorological data was considered in conjunction with GNSS data processing results. Based on the analysis, RMS and coordinate differences were determined and examined. The meteorological data variations should be used for improving PPP positioning accuracy.

1. Introduction

Global Navigation Positioning Systems (GNSS/GPS) methods are widely used for horizontal and vertical positioning in many applications throughout the world. Static, kinematic, differential, real-time kinematic (RTK), precise point processing (PPP), network RTK and similar satellite positioning methods have been developed and used from 1970 up to the present day.

Today, Precise Point Positioning (PPP) is a developing technique that it is currently being studied by many researchers and scientists. PPP was first developed for static applications [1]. The aim of the PPP technique is to process measurements from a single GNSS receiver in order to compute a highly accurate position in a global reference frame. Such a position is made available through the combined products in the form of an IGS orbit/clock [1–3]. With the development of final, near-real-time, or real-time satellite orbit and clock products, kinematic PPP is being increasingly used in research and in various engineering and other applications.

There are several scientific researches reported in the literature and some of them are given that we consider in this paper. Xiang et al. [4] compared the PPP models with the smoothed code method to assess the degree of bias consistency, and to investigate the biases in the ionospheric observables. Mohammed et al. [5] examined the achievable repeatability and accuracy assessment of PPP daily solutions when using GPS only (PPP GPS), GLONASS only (PPP GLO), and GPS plus GLONASS (PPP GPS + GLO) for static positioning. Alkan et al. [6] also investigated the usability of the PPP technique in urban areas with GPS-only and GPS + GLONASS data by the use of online-PPP services for sub-decimeter surveying applications. Cai et al. [7], investigated the quad-constellation PPP for position determination and for analysing its positioning performance, and compared the solutions determined by GPS-only, BeiDou-only, GPS/BeiDou, GPS/GLONASS and GPS/BeiDou/GLONASS, using datasets collected at five stations over sixteen consecutive days. Doğan et al. [8] investigated the accuracy of GPS positioning in terms of seasonal variations depending on baseline lengths using the post-processing method. Anqule et al. [9] studied the resolution of GPS carrier-phase ambiguities in PPP using daily observations. Şanlı and Kurumahmut [10] studied the accuracy of GPS positioning in the presence of large height differences as determined by the PPP method using GIPSY/Oasis. Geng et al. [11] studied Ambiguity Resolution using PPP with hourly data. Ge et al. [12] studied the resolution of GPS carrier-phase ambiguities in PPP using daily observations. Chen and Gao [13] investigated PPP using single-frequency data which would be of interest to a broad range of applications, as the majority of GPS users use single-frequency GPS receivers. Van Bree and Tiberius [14], studied the performance of real-time single-frequency PPP in terms of position accuracy. Abd Rabbou and El-Rabbany [15] compared three kinematic PPP solutions, namely standalone GPS,

E-mail address: oaykut@yildiz.edu.tr.

https://doi.org/10.1016/j.measurement.2018.03.027
Received 21 April 2017; Received in revised form 10 March 2018; Accepted 12 March 2018
Available online 14 March 2018

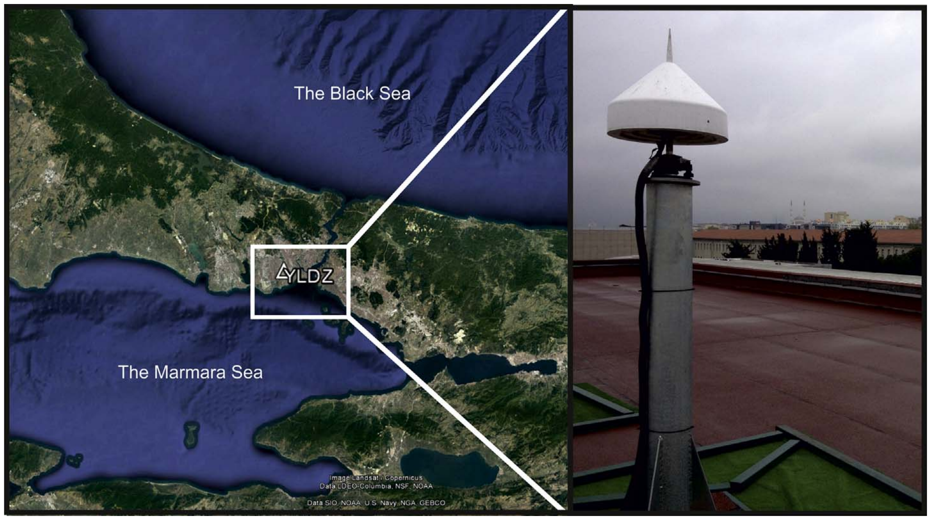

Fig. 1. The location of the YLDZ reference station.

Table 1
Cartesian coordinates and velocities of YLDZ point [20].

X (m)	Y (m)	Z (m)	vx (m)	vy (m)	vz (m)
4219315.141	2328105.672	4164453.864	−0.0179	0.0151	0.0083

standalone GLONASS, and combined GPS/GLONASS solutions. The results also clearly showed that the addition of GLONASS satellites observations generally improved the positioning accuracy compared to GPS only PPP. Teunissen and Khodabandeh [16] determined analytical expressions for the variance matrices of the ambiguity-fixed and ambiguity float PPP-RTK corrections. The PPP-RTK technique is integer ambiguity resolution-enabled PPP. PPP-RTK extends the PPP concept by providing single-receiver users, next to the orbits and clocks, also information about the satellite phase biases [16].

By using a dual-frequency GNSS receiver, PPP has been widely demonstrated to be capable of providing accurate position solutions at the sub-centimeter level for static positioning with the support of precise satellite orbits and clocks [1,17,18]. The ionospheric-free combinations of dual-frequency GNSS pseudo-range (P) and carrier-phase observations (φ) are related to the user position, clock, troposphere and ambiguity parameters, according to the following simplified observation equations [2,17,19]:

$$l_P = \rho + c(dt - dT) + T_r + \varepsilon_P \quad (1)$$

$$l_\Phi = \rho + c(dt - dT) + T_r + N\lambda + \varepsilon_\Phi \quad (2)$$

In Eqs. (1) and (2), l_P is the ionosphere-free combination of L1 and L2 pseudo-ranges; l_Φ is the ionosphere-free combination of the L1 and L2 carrier-phases; ρ is the geometrical range between satellite and station; C is the vacuum speed of light, dt is the station clock offset from GPS time; *dT* is the satellite clock offset from GPS time; *Tr* is the signal path delay due to primarily the troposphere, λ is the carrier, or carrier-combination wavelength; *N* is the ambiguity of the carrier-phase ionosphere-free combination; ε_P *and* ε_Φ are the relevant measurement noise components, including multipath. Given precise estimates of GPS satellite orbits and clocks, Eqs. (1) and (2) reduce to the following equations [17,19]:

$$l_P = \rho + c\ dT + M\ zpd + \epsilon_P \quad (3)$$

$$l_\Phi = \rho + c\ dT + M\ zpd + N\ \lambda + \epsilon_\Phi \quad (4)$$

Linearization of observation Eqs. (3) and (4) around the a priori parameters and observations (X_0,l) becomes Eq. (5), where A is the design matrix, δ is the vector of corrections to unknown parameters X, W is the misclosure vector and V is the vector of residuals.

$$A\delta + W - V = 0 \quad (5)$$

The partial derivatives of the observation equations with respect to the vector of unknown parameters X, containing station position (x, y, z), clock (dt), troposphere zenith total delay (ztd) and real-valued carrier-phase ambiguities (N), form A which is the design matrix. The least squares solution with a priori weighted parameter constraints (Px) is given in Eq. (6) [17,19]:

$$\delta = -\left(P_{X^0} + A^T P_l A\right)^{-1} A^T P_l W \quad (6)$$

The estimated parameters (Eq. (7)) are given with covariance matrix with Eq. (8).

$$\hat{X} = X^0 + \delta \quad (7)$$

$$C_{\hat{X}} = P_{\hat{X}}^{-1} = \left(P_{X^0} + A^T P_l A\right)^{-1} \quad (8)$$

The PPP-GNSS method has become increasingly useful for

Table 2
GPS days of processed GNSS data (2014).

Months	Jan	Feb	Mar	Apr	May	July	June	Aug	Sep	Oct	Nov	Dec
GPS Days of 2014	25	47	74	105	135	166	196	227	258	288	320	349
	26	48	75	106	136	167	197	228	259	289	321	350
	27	50	76	107	138	168	198	229	260	290	323	351